Assessment of Laser Effects on the Structure and Electrical Properties of the Compound $Bi_{2-x}Ag_xSr_2Ca_2Cu_3O_{10+\delta}$ Superconducting

Nihad Ali Shafeek[1*]

Abstract

This research contains preparing the superconducting compound $Bi_{2-x}Ag_xSr_2Ca_2Cu_3O_{10+\delta}$ and studying its structural and electrical characteristics. The samples were prepared using the solid-state method in two stages, and different concentrations of x were (x= 0.2,0.4,0.6,0.8) replaced instead of bismuth Bi. Then, using a hydraulic press 9 ton/cm^2 and sintering with a temperature of 850°C, the samples were pressed. Next, x-ray diffraction is used to study the structural properties. The study of these samples was presented in different proportions of x values, where x = 0.4 is the best compensation ratio of x. A critical temperature of 140^{0}C and the Tetragonal structure was got. After that, the effect of laser nidinium _ yak (Nd: YAG laser) was used on the compositional. It was found that the temperature value increased, so we got the best critical temperature, which is 142 ^{0}C.

Key Words: Structural Properties, Critical Temperature, Zero Resistivity Point.

DOI Number: 10.14704/nq.2021.19.11.NQ21181 **NeuroQuantology 2021; 19(11):108-115**

Introduction

In 1957, the scientist Bardeen, Cooper, and Schrieffer published the BCS theory (Bardeen, Cooper, & Schrieffer, 1957). A few years later, Josephson's (Josephson, 1962) astonishing predictions regarding the physical properties of inhomogeneous superconductors were announced.

Different crystallographic phases can be exhibited from the tantalum nitride TaNx (e.g., Tetragonal, Hexagonal, and Cubic) (Nie et al., 2001; Terao, 1971).

Pulsed Laser Deposition (PLD) has been used to fabricate it, where 532 nm radiation (the first harmonic) from a Nd_YAG laser (Kawasaki, Namba, & Suda, 2000; Matenoglou et al., 2008). Traditionally, in the PLD, it has been applied with Nd_YAG lasers. Nevertheless, as a demerit, the output power significantly decreases compared to the fundamental 1064 nm radiation. For TaN deposition, this study used High-quality superconducting NbN films (using just the fundamental 1064 nm radiation from an Nd: YAG laser) (Chaudhuri, Nevala, Hakkarainen, Niemi, & Maasilta, 2010), and the same tactic.

The applicability of (PLD) grown Nb films in epitaxial multilayer systems is demonstrated by Haindl et al. (Haindl, Neu, Schultz, & Holzapfel, 2007; Haindl, Weisheit, Neu, Schultz, & Holzapfel, 2007).

Research Method

To get a powder of uniform gray color, appropriate amounts of high purity Bi_2O_3, Ag_2O_3, $Sr(NO_3)_2$, Ca_2CO_3, and CuO powders have been weighed, mixed, and ground in a gate mortar for two hours.

Corresponding author: Nihad Ali Shafeek
Address: 1*Department of Physics, College of Education/Tuzkhurmatu, Tikrit University, Iraq.
1*E-mail: nihadshafeek2016@tu.edu.iq

Relevant conflicts of interest/financial disclosures: The authors declare that the research was conducted in the absence of any commercial or financial relationships that could be construed as a potential conflict of interest.
Received: 09 September 2021 Accepted: 17 October 2021

To make think slurry, the mixture took place by inserting a sufficient quantity of 2_ propanol. Using oven at 80 ºC for 60 min, the mixture is put in a tube furnace. The tube has a programmable controller type Eurotherm 818 for calcinations in the air, which takes out (CO_2 and NO_3) gases from the mixture. For 24 hours and with a heating rate of 5ºC/min, the powder was heated to a temperature of 850ºC. Then, the powder was cooled to 25 ^{0}C. The samples a pellet of (1.4) cm in diameter and (0.2 _ 0.3) cm in thickness, using hydraulic press 9 ton/cm^2 for press samples.

For 24 hours and in an air atmosphere of 850 ºC, the pellets were sintered with a heating rate of 5º C/min. The reason was to ionize the particles of the materials and gradually decrease the volume of pore spaces between them.

At the same rate of heating, the pellets were then cooled to room temperature. Next, regrinding, repressing, and re sintering the sintered pellets were reground. The preparation methods are shown in Figure 1.

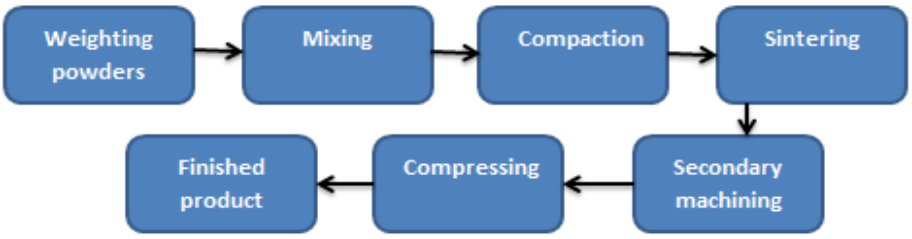

Fig. 1. Schematic Diagram showing preparation of $Bi_{2-x}Ag_xSr_2Ca_2Cu_3O_{10+\delta}$ samples

Tables (1-4) list the weights and compound when x=(0.2,0.4,0.6,0.8)

W1 (Bi_2O_3) = ((2-x)/2)[2(204.37)+3(15.999)] = 456.76

W2(Ag_2O_3)=x/2[2(107.868)+3(15.999)]=263.673 g/mole

W3($Sr(NO_3)_2$ = ((2-x)/2)[(87.62) +2(14.007)+6(15.999)] = 211.628 g/mole

W4 ($CaCO_3$) = [40.078+12.011+3(15.999)] = 100.076 g/mole

W5 ($Cu(NO_3)_2$) = [63.546+2(14.007) + 6(15.999)] = 187.554 g/mole

Table 1. Powder weights for the compound $Bi_{2-x}Ag_xSr_2Ca_2Cu_3O_{10+\delta}$, at x = 0.2

Powder	Weights / 1000	The symbol weight
Bi_2O_3	0.4104	W1
Ag_2O_3	0.0263	W2
$Sr(NO_3)_2$	0. 2116	W3
$CaCO_3$	0.1000	W4
CuO	0.1875	W5

Table 2. Powder weights for the compound $Bi_{2-x}Ag_xSr_2Ca_2Cu_3O_{10+\delta}$, at x = 0.4

Powder	Weights / 1000	The symbol weight
Bi_2O_3	0.36448	W1
Ag_2O_3	0.0527346	W2
$Sr(NO_3)_2$	0. 2116	W3
$CaCO_3$	0.1000	W4
CuO	0.1875	W5

Table 3. Powder weights for the compound $Bi_{2-x}Ag_xSr_2Ca_2Cu_3O_{10+\delta}$, at x = 0.6

Powder	Weights / 1000	The symbol weight
Bi_2O_3	0.3192	W1
Ag_2O_3	0.0791019	W2
$Sr(NO_3)_2$	0. 2116	W3
$CaCO_3$	0.10000	W4
CuO	0.1875	W5

Table 4. Powder weights for the compound $Bi_{2-x}Ag_xSr_2Ca_2Cu_3O_{10+\delta}$, at x = 0.8

Powder	Weights / 1000	The symbol weight
Bi_2O_3	0.2736	W1
Ag_2O_3	0.1054692	W2
$Sr(NO_3)_2$	0. 2116	W3
$CaCO_3$	0.1000	W4
CuO	0.1875	W5

Objective of the Research

The object of this study is to obtain the impact of the partial compensation of the silver element (Ag) on the Bizmoth element (Bi) on the structural and electrical properties. Additionally, to determine the impact of the nidemium yak laser on the properties improvement of $Bi_{2-x}Ag_xSr_2Ca_2Cu_3O_{10+\delta}$ superconducting.

Results and Discussion

The mixture is then placed in the x-ray machine to obtain x-ray diffraction and measure the angles of the different reflections and then obtain the crystalline composition of the sample. If the relationship is achieved a = b ≠ c means that it has a tetragonal structure, which possesses superconductivity properties (Galy, 1989; Goldstein et al., 2017).

X-ray diffraction has been used to test the prepared samples' structure.

Source: Cupper Kα

Wavelength: (1.5405 A⁰)

Current: (20 mA)

Voltage: (40 KV)

A Basic Language (Al-Shakarchi, 1997) was worked out to find the lattice parameters (a,b,c), where the language is based on Cohen's least. Here, an x-ray of wavelength λ is considered as an incident at an angle Θ on two parallel planes of atoms (separated by interference). If Bragg's law is satisfied, then:

$$2d\sin\Theta = n\lambda \quad (1)$$

Where (Θ) denotes the angle between the incident beam of x-ray and plane. Additionally, the distance between two parallel planes of atoms is represented (d) (which is interplanar spacing d_{hkl}). The wavelength of the incident x-ray and the reflection order are symbolized as (λ, and n), respectively.

This work considered that (λ)is fixed using a cobalt source or cooper (for cooper source n=1 and λ=1.54056 A⁰)

The peak position in the diffraction pattern is used to calculate the angle Θ. Then, d is determined using Equation (1). A set of Miller indices (h k l) is associated with each value. Equation (2) is used to calculate the lattice parameters(a,b,c) (Callister & Rethwisch, 2011).

$$\frac{1}{d^2} = \frac{h^2}{a^2} + \frac{k^2}{b^2} + \frac{l^2}{c^2} \quad (2)$$

A powder of these samples was used. A computer controller diffractometer is used to the data. As illustrated in Figure (2-5), the solid-state reaction is used to prepare the findings of the type 2223, $Bi_{2-x}Ag_xSr_2Ca_2Cu_3O_{10+\delta}$ systems.

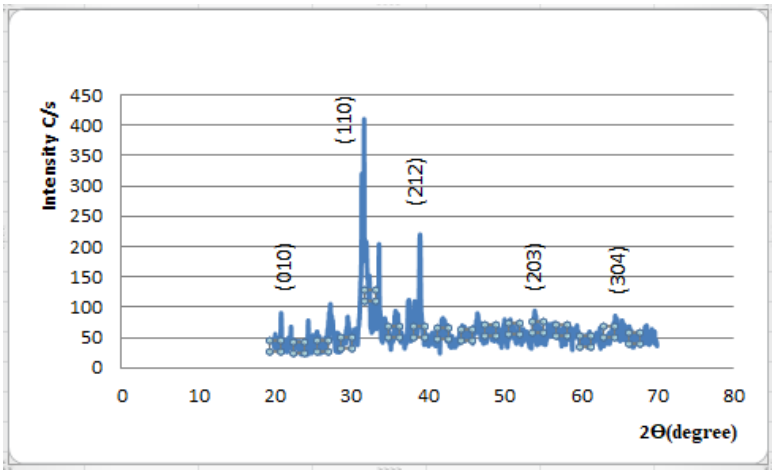

Fig. 2. The powder X-ray diffraction of $Bi_{2-x}Ag_xSr_2Ca_2Cu_3O_{10+\delta}$ sample for x= 0.2

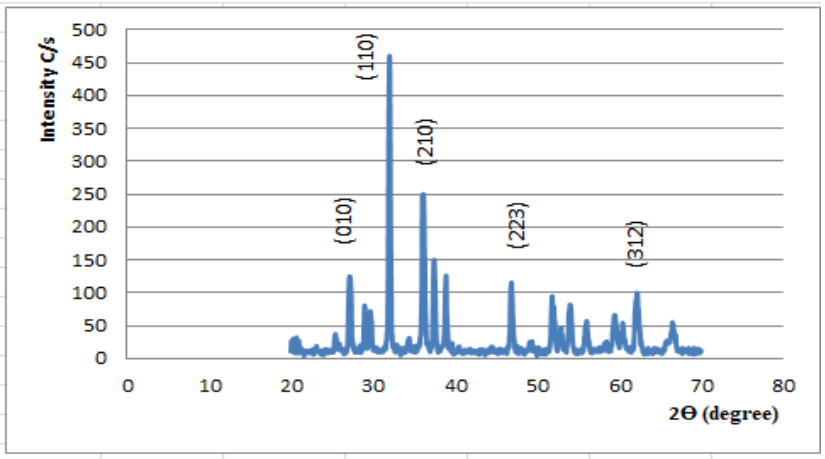

Fig. 3. The powder X-ray diffraction of $Bi_{2-x}Ag_xSr_2Ca_2Cu_3O_{10+\delta}$ sample for x= 0.4

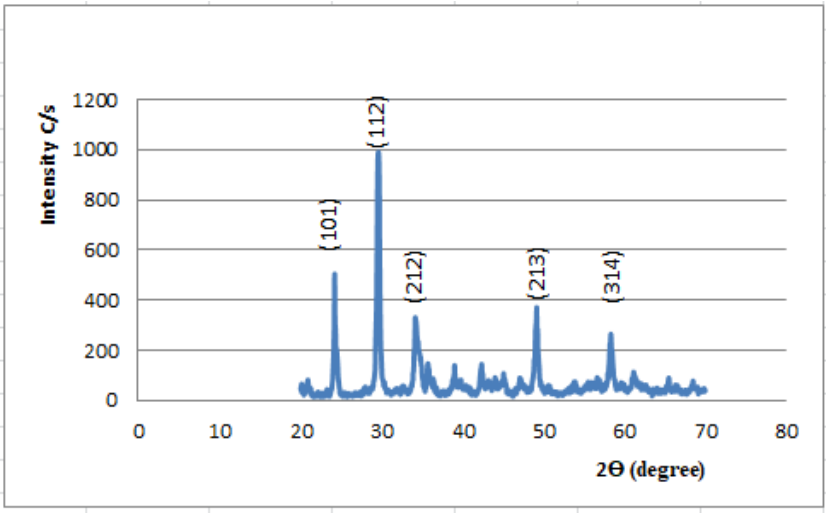

Fig. 4. The powder x-ray diffraction of $Bi_{2-x}Ag_xSr_2Ca_2Cu_3O_{10+\delta}$ sample for x= 0.6

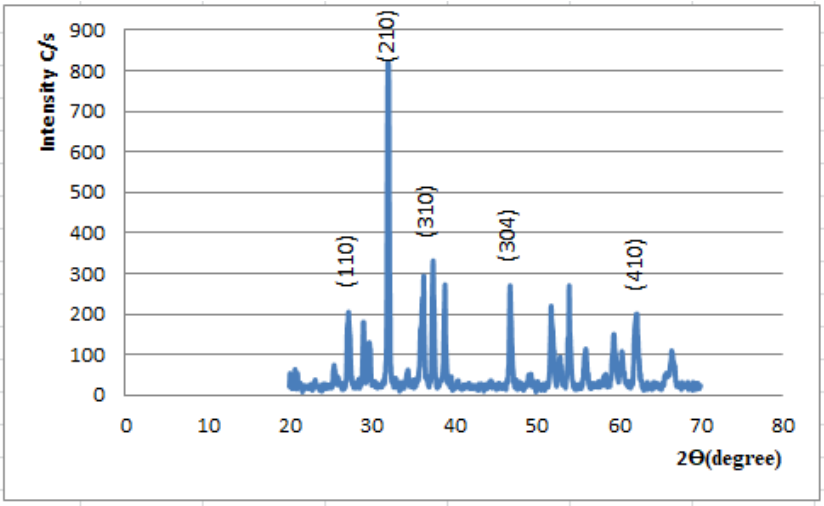

Fig. 5. The powder X-ray diffraction of $Bi_{2-x}Ag_xSr_2Ca_2Cu_3O_{10+\delta}$ sample for x= 0.8

From the figure, we can calculate the value of (d) by using equation (1) and calculate the value of (a,b,c) from equation (2), outlined in Table (5).

Table 5. The value of (h k l) and (d), (a,b,c) for compound $Bi_{2-x}Ag_xSr_2Ca_2Cu_3O_{10+\delta}$ at x= (0.2,0.4,0.6,0.8)

Ratio of x	h k l	d / A⁰	a=b / A⁰	C / A⁰
0.2	1 1 0	2.7907	3.928	33.36
0.4	1 1 0	2.8422	4.12	32.94
0.6	1 1 2	3.0105	4.23	32.08
0.8	2 1 0	2.7902	4.05	33.21

Resistivity and Critical Temperature Measurement

A four-point probe is the most common method to determine the T_c of superconductivity (Wu et al., 1987). The curve in Figure (9) is used to determine Tc (critical temperature). The resistivity of Tc comprises of two parameters: Tc1 (transition) and Tc2 (zero resistivity point) (Eckroad, 2009; John & Fredrich, 2010). It can be calculated as follows.

$$Tc = ((Tc1+Tc2) / 2) \quad (3)$$

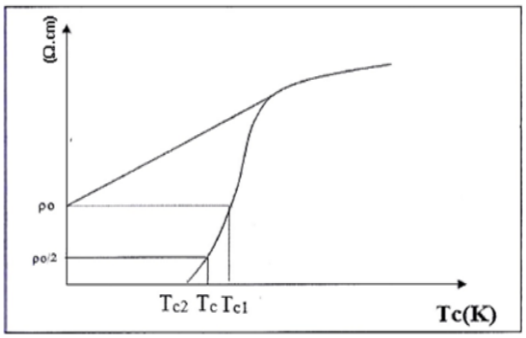

Figure 6. Measurement of the resistivity (to calculate Tc).

Before laser irradiation, Figure (7) refers the resistivity vs temperature of compound $Bi_{2-x}Ag_xSr_2Ca_2Cu_3O_{10+\delta}$ at x=0.2 obtains a value of T_c=119 K. Additionally, Figure (8) illustrates the resistivity vs temperature of compound $Bi_{2-x}Ag_xSr_2Ca_2Cu_3O_{10+\delta}$ at x= 0.4 reveals a value of T_c=129K. Similarlly, Figure (9) presents the resistivity vs temperature of compound $Bi_{2-x}Ag_xSr_2Ca_2Cu_3O_{10+\delta}$ at x = 0.6 determine a best value of T_c = 140 K. Accordinglly, Figure (10) draws the resistivity vs temperature of compound $Bi_{2-x}Ag_xSr_2Ca_2Cu_3O_{10+\delta}$ at x = 0.8 gives a value of T_c = 125 K.

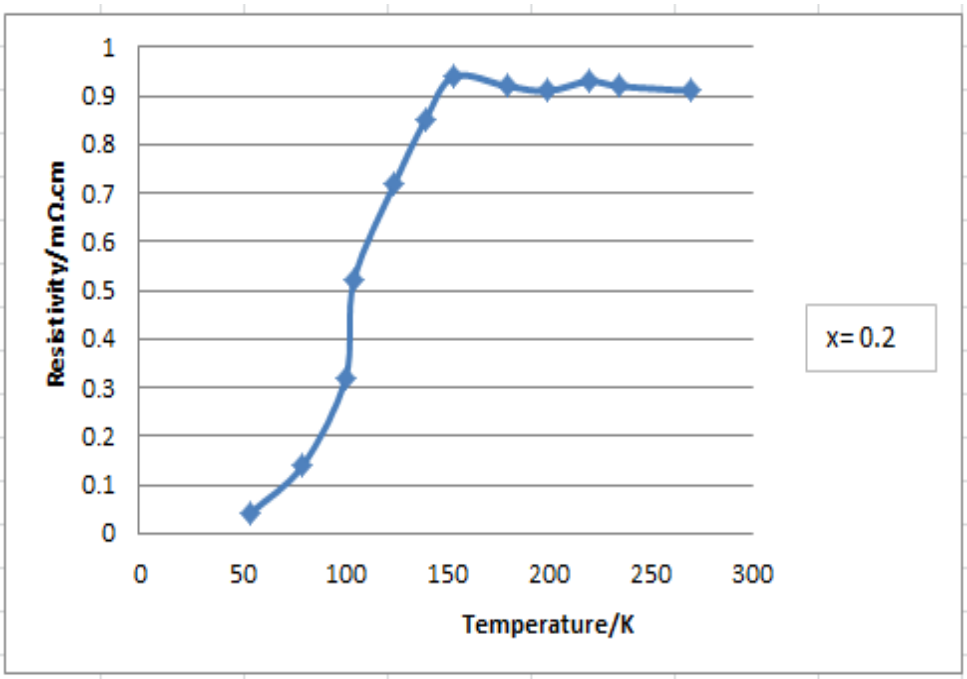

Figure 7. The resistivity with temperature of $Bi_{2-x}Ag_xSr_2Ca_2Cu_3O_{10+\delta}$, at x = 0.2 (before laser irradiation).

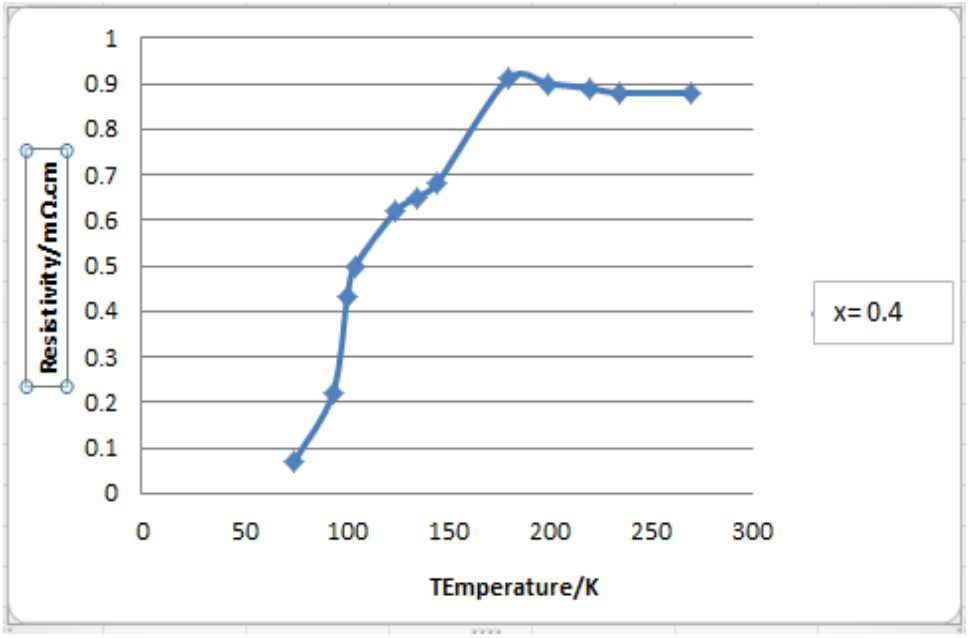

Figure 8. The resistivity with temperature of $Bi_{2-x}Ag_xSr_2Ca_2Cu_3O_{10+\delta}$, at x = 0.4 (before laser irradiation)

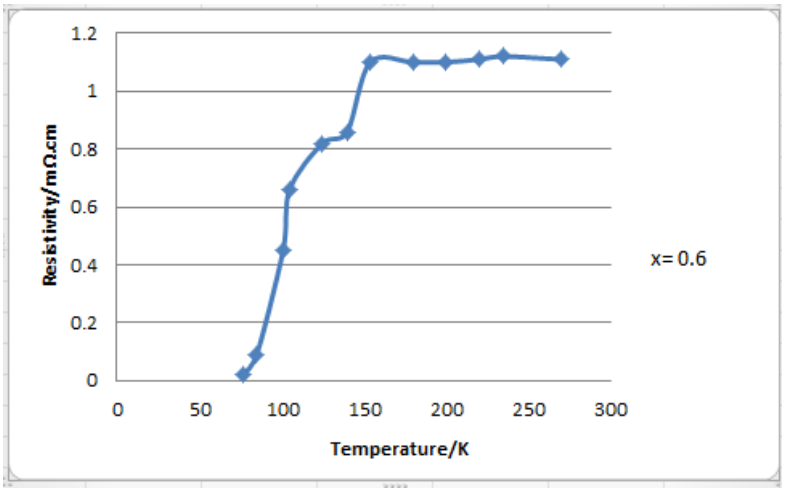

Figure 9. The resistivity with temperature of $Bi_{2-x}Ag_xSr_2Ca_2Cu_3O_{10+\delta}$, at x = 0.6 (before laser irradiation)

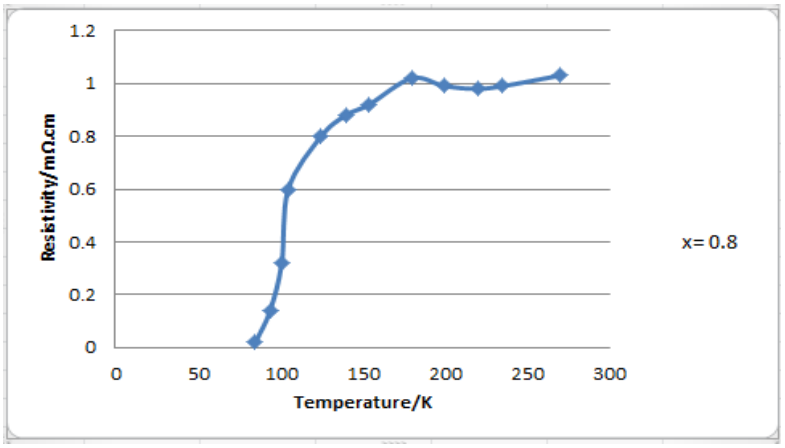

Figure 10. The resistivity with temperature of $Bi_{2-x}Ag_xSr_2Ca_2Cu_3O_{10+\delta}$, at x = 0.8 (before laser irradiation)

Similar to above, however, after laser irradiation, Figure (11) refers the resistivity vs temperature of compound $Bi_{2-x}Ag_xSr_2Ca_2Cu_3O_{10+\delta}$ at x = 0.2 reveals a value of T_c=121 K. Additionally, Figure (12) illustrates the resistivity vs temperature of compound $Bi_{2-x}Ag_xSr_2Ca_2Cu_3O_{10+\delta}$ at x = 0.4 obatins a value of T_c = 131 K. Similarlly, Figure (13) presents the resistivity vs temperature of compound $Bi_{2-x}Ag_xSr_2Ca_2Cu_3O_{10+\delta}$ at x = 0.6 shows a best value of T_c = 142 K. Accordinglly, Figure (14) determines the resistivity vs temperature of compound $Bi_{2-x}Ag_xSr_2Ca_2Cu_3O_{10+\delta}$ at x = 0.8 obtain a value of T_c=127 K.

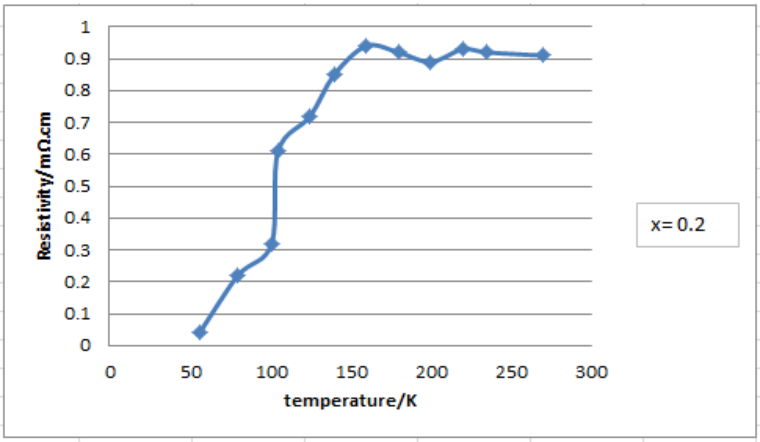

Figure 11. The resistivity with temperature of $Bi_{2-x}Ag_xSr_2Ca_2Cu_3O_{10+\delta}$, at x = 0.2 (after laser irradiation)

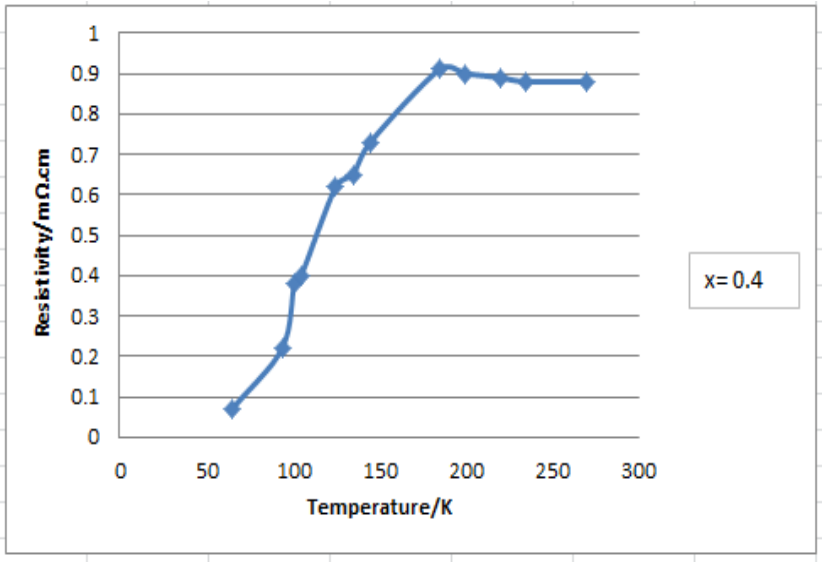

Figure 12. The resistivity with temperature of $Bi_{2-x}Ag_xSr_2Ca_2Cu_3O_{10+\delta}$, at x = 0.4 (after laser irradiation)

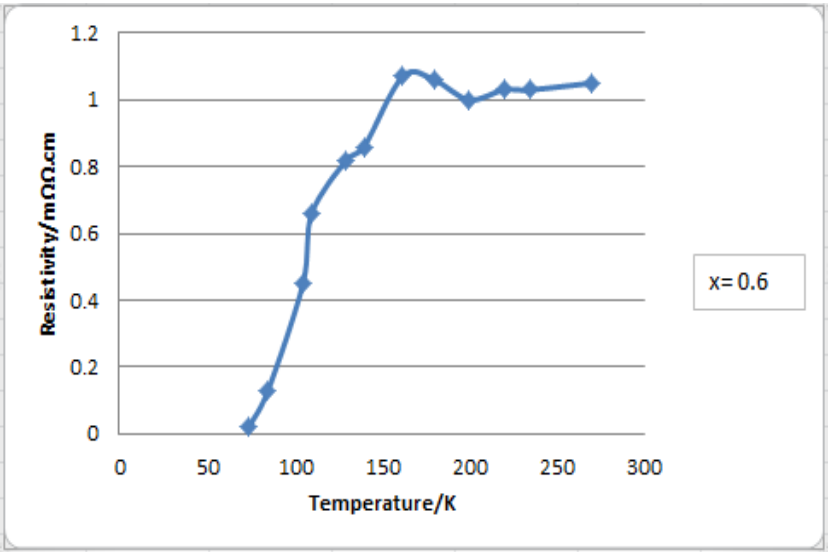

Figure 13. The resistivity with temperature of $Bi_{2-x}Ag_xSr_2Ca_2Cu_3O_{10+\delta}$, at x = 0.6 (after laser irradiation)

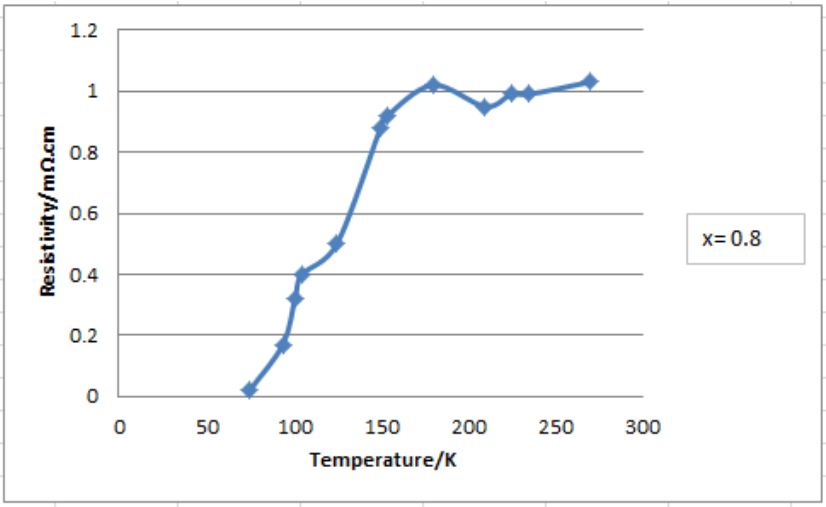

Figure 14. The resistivity with temperature of $Bi_{2-x}Ag_xSr_2Ca_2Cu_3O_{10+\delta}$, at x = 0.8 (after laser irradiation)

*e*ISSN 1303-5150

Table 6. Average critical temperature and grains diameter of x = 0.3,0.6,0.9,1.2 of compound $Bi_{2-x}Ag_xSr_2Ca_2Cu_3O_{10+\delta}$

The ratio of (x)	Critical Temperature (T_c)	
	Before laser irradiation	After laser irradiation
0.2	119 K	121K
0.4	129 K	131 K
0.6	140 K	142 k
0.8	127 K	132K

Conclusion

XRD pattern has shown the tetragonal structure, and the substitution Ag instate of Bi for compound $Bi_{2-x}Ag_xSr_2Ca_2Cu_3O_{10+\delta}$ give a best value of T_c = 140 K at x = 0.6 (before laser irradiation). Whereas, after laser irradiation shows the increasing value of T_c = 142 k, t is better to use laser irradiation when preparing superconducting samples or to use nanoparticles of silver Ag.

References

Al-Shakarchi EK. The Variation of the structure and phase Transformation in Y-Ba-Cu-O High Temperature Superconductor Compound with Isovalent Substitution. *University of Baghdad* 1997.

Bardeen J, Cooper LN, Schrieffer JR. Theory of superconductivity. *Physical review* 1957: 108(5).

Callister WD, Rethwisch DG. *Materials science and engineering.* John wiley & sons New York 2001: 5.

Chaudhuri S, Nevala M, Hakkarainen T, Niemi T, Maasilta I. Infrared pulsed laser deposition of niobium nitride thin films. *IEEE transactions on applied superconductivity* 2010; 21(3): 143-146.

Eckroad S. Program on technology innovation: a superconducting DC cable. *Electric Power Research Institute, Final Report* 2009: 1020458.

Galy J. *Solid State Chemistry.* 1989.

Goldstein JI, Newbury DE, Michael JR, Ritchie NW, Scott JHJ, Joy DC. *Scanning electron microscopy and X-ray microanalysis:* Springer 2017.

Haindl S, Neu V, Schultz L, Holzapfel B. Nb/SmCo5 bilayers prepared by UHV–pulsed laser deposition. *Physica C: Superconductivity* 2007; 460: 1390-1391.

Haindl S, Weisheit M, Neu V, Schultz L, Holzapfel B. Epitaxial heterostructures of hard magnetic and superconducting thin films. *Physica C: Superconductivity and its applications* 2007; 463: 1001-1004.

John B, Fredrich M. *The development of SQUID-based gradiometere.* MSC thesis. Stellenbosch University 2010.

Josephson BD. Possible new effects in superconductive tunnelling. Physics letters 1962; 1(7): 251-253.

Kawasaki H, Namba KDJ, Suda Y. Tantalum nitride thin films synthesized by pulsed Nd: YAG laser deposition method. *MRS Online Proceedings Library (OPL)* 2000: 617.

Matenoglou G, Koutsokeras L, Lekka CE, Abadias G, Camelio S, Evangelakis GA, Patsalas P. Optical properties, structural parameters, and bonding of highly textured rocksalt tantalum nitride films. *Journal of applied physics* 2008; 104(12).

Nie H, Xu S, Wang S, You L, Yang Z, Ong C, Liew T. Structural and electrical properties of tantalum nitride thin films fabricated by using reactive radio-frequency magnetron sputtering. *Applied Physics A* 2001; 73(2): 229-236.

Terao, N. (1971). Structure of tantalum nitrides. *Japanese Journal of Applied Physics* 1971: 10(2).

Wu MK, Ashburn JR, Torng C, Hor PH, Meng RL, Gao L, Chu A. Superconductivity at 93 K in a new mixed-phase Y-Ba-Cu-O compound system at ambient pressure. *Physical review letters* 1987; 58(9).

Radhi AH, Du EAB, Khazaal FA, Abbas ZM, Aljelawi OH, Hamadan SD, Almashhadani HA, Kadhim MM. HOMO-LUMO energies and geometrical structures effecton corrosion inhibition for organic compounds predict by DFT and PM_3 methods. *NeuroQuantology* 2020; 18(1): 37-45.